"Classical" Self-Consistent Nuclear Model. II

R. G. SEYLER
Department of Physics and Astronomy, The Ohio State University, Columbus, Ohio

AND

C. H. BLANCHARD
Department of Physics, The University of Wisconsin, Madison, Wisconsin

(Received 25 February 1963)

The gross energetics and sizes of the stable nuclei are accurately reproduced by a simple model of nuclear structure using Thomas-Fermi approximation. Saturation is obtained by taking the (spatially Yukawa) two-body interaction to be (quadratically) momentum-dependent. Coulomb effects and neutron-proton mass difference are included. The two coupled nonlinear integral equations for neutron and proton spatial distributions are integrated. The system of equations is made unique by the choice of only four input parameters, and these parameters are optimized by requiring a best fit of the solution to the binding-energy-per-nucleon and neutron-proton-ratio curves as a function of A. The optimum parameter values are reasonable. The Yukawa force range is found to be about 40% of $\hbar/(m_\pi c)$. A small but definite excess of neutron radius over proton radius is found, and also a slight depression of the central proton density for the heavier nuclei. Satisfactory agreement with measured radii and surface thicknesses is obtained.

INTRODUCTION

EARLIER work,[1] hereafter referred to as I, investigated a degenerate-fermion-gas nuclear model in "classical" (Thomas-Fermi) approximation.[2] Two-body forces were assumed, with a Yukawa dependence on relative position and, to produce saturation, a quadratic[3] dependence on relative momentum. In I it was found that the integral equation for the spatial distribution of nucleons could be solved; and that a saturated inner region of the nucleus and a surface region of the correct sizes are predicted for reasonable values of the input parameters. We here report on an extension, involving interpenetrating neutron and proton distributions, to take into account Coulomb effects and produce a realistic nuclear model.

We regard the neutrons (protons) in the ground state of a nucleus as a degenerate gas. At each point of configuration space, neutron (proton) momentum space is assumed to be filled as densely as allowed by the Pauli principle: two neutrons (protons) per momentum state, up to the Fermi momentum for the neutrons, p_{Fn} (protons, p_{Fp}). We consider only spherical nuclei, in which case the Fermi momenta depend only on the distance $r(=|\mathbf{r}|)$ from the center of the nucleus: $p_{Fn}=p_{Fn}(r)$ and $p_{Fp}=p_{Fp}(r)$. The total nucleon spatial density will be the sum of the neutron and proton densities,

$$n(r)=n_n(r)+n_p(r), \tag{1a}$$

where

$$n_n(r)=2(2\pi\hbar)^{-3}(4\pi/3)[p_{Fn}(r)]^3, \tag{1b}$$

and

$$n_p(r)=2(2\pi\hbar)^{-3}(4\pi/3)[p_{Fp}(r)]^3. \tag{1c}$$

Since we assume that the two-body interaction is momentum-dependent, our model will give a momentum-dependent nucleon-nucleus potential energy function[4] (momentum-dependent optical-model potential[5]). We introduce an average (over the spin states occurring) nuclear interaction, which, in spite of the presumed charge independence of nuclear forces, can be expected to be of different strength for the unlike (np) and like (nn and pp) interactions.

To calculate the potential energy of a neutron with momentum $\mathbf{p}$ at the position $\mathbf{r}$, one must *first* add the energy contributions of the neutrons' interaction with all those neutrons having momenta within the Fermi neutron sphere (FNS) at $\mathbf{r}'$, and the contributions of the neutrons' interaction with all those protons having momenta within the Fermi proton sphere (FPS) at $\mathbf{r}'$, and *second* add the contributions from different $\mathbf{r}'$ throughout the nuclear volume (NV):

$$U_n(\mathbf{r},\mathbf{p})=-U_0\int_{\mathrm{NV}}F\left(\left|\frac{\mathbf{r}-\mathbf{r}'}{r_D}\right|\right)\frac{2}{(2\pi\hbar)^3}\times\left\{\int_{\mathrm{FNS}}d\mathbf{p}'G\left(\left|\frac{\mathbf{p}-\mathbf{p}'}{p_D}\right|\right)+k\int_{\mathrm{FPS}}d\mathbf{p}'G\left(\left|\frac{\mathbf{p}-\mathbf{p}'}{p_D}\right|\right)\right\}d\mathbf{r}', \tag{2}$$

where U_0 is a fixed positive energy giving the strength of the like-nucleon interaction and k is the ratio of the unlike to like interaction. Thus, kU_0 is the strength of

[1] R. G. Seyler and C. H. Blanchard, Phys. Rev. **124**, 227 (1961).
[2] Application of "the" Thomas-Fermi method to nuclear structure has been varied and largely confined to studies of the nuclear surface. Work closely related to the present work is reported by Y. Hara [Progr. Theoret. Phys. (Kyoto) **24**, 1179 (1960)] whose paper refers to most of the previous nuclear-structure work in Thomas-Fermi approximation.
[3] J. S. Bell, in *Lecture Notes on the Many Body Problem*, edited by C. Fronsdal (W. A. Benjamin, Inc., New York, 1962) has shown that it is possible to eliminate the hard-core part of a two-body interaction in favor of a quadratically momentum-dependent interaction (plus many-body corrections, which we do not consider here).
[4] V. F. Weisskopf, Nucl. Phys. **3**, 423 (1957).
[5] F. Perey and B. Buck, Nucl. Phys. **32**, 353 (1962).

the np interaction. The function G expresses the momentum dependence of the interaction, the function F the spatial dependence, and r_D and p_D are, respectively, length and momentum parameters introduced to make the arguments of F and G dimensionless.

The potential energy of a proton with momentum $\mathbf{p}$ at position $\mathbf{r}$ is

$$U_p(\mathbf{r},\mathbf{p})=-U_0\int_{\mathrm{NV}}d\mathbf{r}'F\left(\left|\frac{\mathbf{r}-\mathbf{r}'}{r_D}\right|\right)\frac{2}{(2\pi\hbar)^3}\times\left\{k\int_{\mathrm{FNS}}d\mathbf{p}'G\left(\left|\frac{\mathbf{p}-\mathbf{p}'}{p_D}\right|\right)+\int_{\mathrm{FPS}}d\mathbf{p}'G\left(\left|\frac{\mathbf{p}-\mathbf{p}'}{p_D}\right|\right)\right\}+\int_{\mathrm{NV}}d\mathbf{r}'\frac{e^2}{|\mathbf{r}-\mathbf{r}'|}\frac{2}{(2\pi\hbar)^3}\int_{\mathrm{FPS}}d\mathbf{p}', \quad (3)$$

where the last term is the Coulomb potential energy (e=proton charge), and r_D and p_D are the ranges of the interaction in configuration and momentum space.

We adopt, as in I, for F, the Yukawa function,

$$F(x)=e^{-x}/x, \quad (4)$$

and for G, the quadratic,

$$G(x)=1-x^2. \quad (5)$$

The choice of a quadratic for G leads to a spatially dependent effective-mass approximation. Levinger and his co-workers[6] have employed a quadratically momentum-dependent potential to describe the two-nucleon singlet-even scattering data and have concluded that the resultant description is as accurate as any based on a "hard-core" potential model. The equations we derive should, in the limit of infinite nuclear volume and with the neglect of the Coulomb repulsion and np mass difference, describe "nuclear matter" and will, in fact, reduce to the constant effective-mass approximation which has been examined by Weisskopf[4] and Mittelstaedt.[7]

BASIC EQUATIONS

We seek the distribution in space of the nucleons in the ground state of a spherical nucleus. Our approach is to look for a distribution which will minimize the total energy, E_T, of a nucleus, subject to the condition that the total number of nucleons, $A=N+Z$, be fixed.

We have

$$N=\int_{\mathrm{NV}}d\mathbf{r}\int_{\mathrm{FNS}}d\mathbf{p}\frac{2}{(2\pi\hbar)^3}, \quad (6)$$

$$Z=\int_{\mathrm{NV}}d\mathbf{r}\int_{\mathrm{FPS}}d\mathbf{p}\frac{2}{(2\pi\hbar)^3}, \quad (7)$$

and

$$E_T=\int_{\mathrm{NV}}d\mathbf{r}\frac{2}{(2\pi\hbar)^3}\left[\int_{\mathrm{FNS}}d\mathbf{p}\left\{\frac{p^2}{2M_n}+\tfrac{1}{2}U_n(r,p)\right\}+\int_{\mathrm{FPS}}d\mathbf{p}\left\{\frac{p^2}{2M_p}+\tfrac{1}{2}U_p(r,p)\right\}\right]+NM_nc^2+ZM_pc^2, \quad (8)$$

where U_n and U_p are given by Eqs. (2) and (3). If the neutron-proton mass difference were neglected, as was done in I, the rest energy contribution to the total energy would be a constant, for a given number of nucleons, A, and, therefore, could be omitted from Eq. (8) since its variation would be zero.

Let

$$M\equiv M_n,\qquad \beta\equiv M_n/M_p=1.00138. \quad (9a)$$

Introduce the dimensionless quantities

$$x\equiv r/r_D,\qquad x_0=R/r_D, \quad (9b)$$

where R is the radius of the nucleon distribution,[8] and

$$\varphi(x)\equiv p_{Fn}(r)/p_D,\qquad \psi(x)\equiv p_{Fp}(r)/p_D. \quad (10a)$$

Let

$$C_N\equiv\frac{2}{3\pi}\frac{U_0}{(p_D^2/2M)}\left(\frac{r_Dp_D}{\hbar}\right)^3,\qquad C_C\equiv\frac{4}{3\pi}\frac{e^2/r_D}{(p_D^2/2M)}\left(\frac{r_Dp_D}{\hbar}\right)^3, \quad (10b)$$

where the subscripts N and C refer to "nuclear" and "Coulomb," respectively.

Carrying out the integrations in Eqs. (6), (7), and (8) as far as possible for arbitrary φ and ψ we find for N, Z, and E_T as functionals of $\varphi(x)$ and $\psi(x)$

$$N=\frac{4}{3\pi}\left(\frac{r_Dp_D}{\hbar}\right)^3\int_0^{x_0}[\varphi(x)]^3x^2dx, \quad (11)$$

$$Z=\frac{4}{3\pi}\left(\frac{r_Dp_D}{\hbar}\right)^3\int_0^{x_0}[\psi(x)]^3x^2dx, \quad (12)$$

[6] M. Razavy, G. Field, and J. S. Levinger, Phys. Rev. **125**, 269 (1962); O. Rojo and L. M. Simmons, *ibid.* **125**, 273 (1962).
[7] P. Mittelstaedt, Nucl. Phys. **8**, 171 (1958).

[8] We argue later that the nucleon density actually achieves the value zero at a finite value of x, which we call x_0 and identify as the nuclear radius.

$$E_T=\frac{4}{3\pi}\left(\frac{r_D p_D}{\hbar}\right)^3\Bigg[\frac{p_D^2}{2M}\Big\{\frac{3}{5}\int_0^{x_0}[\varphi^5(x)+\beta\psi^5(x)]x^2dx-\frac{1}{2}\int_0^{x_0}xdx\Big[C_N\int_0^{x_0}ydy(e^{-|x-y|}-e^{-(x+y)})$$
$$\times\{[\varphi^3(x)+k\psi^3(x)][\varphi^3(y)-\tfrac{3}{5}\varphi^5(y)]+[\psi^3(x)+k\varphi^3(x)][\psi^3(y)-\tfrac{3}{5}\psi^5(y)]-\tfrac{3}{5}\varphi^3(y)[\varphi^5(x)+k\psi^5(x)]$$
$$-\tfrac{3}{5}\psi^3(y)[k\varphi^5(x)+\psi^5(x)]\}+\tfrac{1}{2}C_C\psi^3(x)\int_0^{x_0}ydy\,\psi^3(y)(x+y-|x-y|)\Big]\Big\}$$
$$+Mc^2\left(\int_0^{x_0}\varphi^3(x)x^2dx+\beta^{-1}\int_0^{x_0}\psi^3(x)x^2dx\right)\Bigg]. \quad (13)$$

To minimize E_T while holding A $(=N+Z)$ constant, we introduce a Lagrangian multiplier λ and require

$$\delta[E_T\{\varphi(x),\psi(x)\}-\lambda(N\{\varphi(x),\psi(x)\}+Z\{\varphi(x),\psi(x)\})]=0. \quad (14)$$

This requirement yields, for a variation of φ,

$$x^2\varphi^2(x)\Big\{\varphi^2(x)-\frac{\lambda-Mc^2}{(p_D^2/2M)}-\frac{C_N}{x}\int_0^{x_0}ydy(e^{-|x-y|}-e^{-(x+y)})$$
$$\times\{\varphi^3(y)[1-\tfrac{3}{5}\varphi^2(y)-\varphi^2(x)]-k\psi^3(y)[1-\tfrac{3}{5}\psi^2(y)-\varphi^2(x)]\}\Big\}=0$$

which, after cancelling the common factor $x^2\varphi^2(x)$ gives the nonlinear integral equation linking φ and ψ:

$$\varphi^2(x)=\frac{C_N}{x}\int_0^{x_0}ydy(e^{-|x-y|}-e^{-(x+y)})\times\{\varphi^3(y)[1-\tfrac{3}{5}\varphi^2(y)-\varphi^2(x)]+k\psi^3(y)[1-\tfrac{3}{5}\psi^2(y)-\varphi^2(x)]\}+\frac{\lambda-Mc^2}{p_D^2/2M}. \quad (15)$$

To identify the physical significance of the Lagrangian multiplier λ we rewrite Eq. (15) with the aid of Eq. (2), wherein use is made of the definitions (4), (5), (9), and (10) as

$$\varphi^2(x)=(p_D^2/2M)^{-1}[-U_n(r,p_{Fn})+\lambda-Mc^2],$$

which when solved for λ, use being made of definition (10a), gives

$$\lambda=p_{Fn}^2/2M+U_n(r,p_{Fn})+Mc^2. \quad (16)$$

Recalling that M is the neutron mass we see that λ is the *total* energy of a neutron having momentum $p_{Fn}(r)$, and that this maximum neutron energy is independent of position.

Similarly, variation of ψ in (14) leads after cancelling a common factor $x^2\psi^2(x)$, to

$$\beta\psi^2(x)=\frac{C_N}{x}\int_0^{x_0}ydy(e^{-|x-y|}-e^{-(x+y)})\times\{\psi^3(y)[1-\tfrac{3}{5}\psi^2(y)-\psi^2(x)]+k\varphi^3(y)[1-\tfrac{3}{5}\varphi^2(y)-\psi^2(x)]\}-\frac{C_C}{2x}\int_0^{x_0}\psi^3(y)(x+y-|x-y|)ydy+\frac{\lambda-\beta^{-1}Mc^2}{p_D^2/2M}, \quad (17)$$

which with the aid of Eq. (3) can be solved for λ to give

$$\lambda=\beta p_{Fp}^2/2M+U_p(r,_{Fp})+\beta^{-1}Mc^2. \quad (18)$$

Since M/β is the proton mass, λ is also the total energy of a proton having momentum equal to $p_{Fp}(r)$. Thus, comparing (16) and (18), we have the result that the total energy of the most energetic neutron is exactly equal to the total energy of the most energetic proton. This result insures stability against beta decay.

We introduce the terms Fermi neutron (proton) energy, E_{Fn} (E_{Fp}), as follows:

$$E_{Fn}\equiv\lambda-Mc^2=p_{Fn}^2/2M+U_n(r,p_{Fn}),$$
$$E_{Fp}\equiv\lambda-\beta^{-1}Mc^2=\beta p_{Fp}^2/2M+U_p(r,p_{Fp}). \quad (19a)$$

Thus, E_{Fn}, for example, is the total energy minus the rest energy of the most energetic neutron or, equivalently, from (16), the sum of the kinetic and potential energies of the most energetic neutron. (E_{Fn} should not be confused with the Fermi neutron *kinetic* energy, T_{Fn}, which is the term $p_{Fn}^2/2M$.)

We define two additional dimensionless quantities

$$\epsilon_{Fn}\equiv E_{Fn}/(p_D^2/2M),$$
$$\epsilon_{Fp}\equiv E_{Fp}/(p_D^2/2M), \quad (19b)$$

and rewrite Eqs. (15) and (17) as

$$\varphi^2(x)=\frac{\frac{C_N}{x}\int_0^{x_0}(e^{-|x-y|}-e^{-(x+y)})\{\varphi^3(y)[1-\tfrac{3}{5}\varphi^2(y)]+k\psi^3(y)[1-\tfrac{3}{5}\psi^2(y)]\}ydy+\epsilon_{Fn}}{\frac{C_N}{x}\int_0^{x_0}(e^{-|x-y|}-e^{-(x+y)})[\varphi^3(y)+k\psi^3(y)]+1}, \quad (20)$$

and

$$\psi^2(x)=\frac{\dfrac{C_N}{x}\displaystyle\int_0^{x_0}(e^{-|x-y|}-e^{-(x+y)})\{\psi^3(y)[1-\tfrac{3}{5}\psi^2(y)]+k\varphi^3(y)[1-\tfrac{3}{5}\varphi^2(y)]\}ydy+\epsilon_{Fp}}{\dfrac{C_N}{x}\displaystyle\int_0^{x_0}(e^{-|x-y|}-e^{-(x+y)})[\psi^3(y)+k\varphi^3(y)]+\beta} \left.\vphantom{\frac{1}{1}}\right\} \quad (21)$$
$$-\frac{\dfrac{C_C}{2x}\displaystyle\int_0^{x_0}\psi^3(y)(x+y-|x-y|)ydy}{\text{(Same denominator)}}\Bigg\}.$$

These two coupled equations are our basic working equations. Their solutions determine, through the use of Eqs. (10) and (1), the nucleon density distribution.

Physically, x_0 is the distance (measured in units of r_D) beyond which the nucleon density is zero. Thus, to be physically reasonable both $\varphi(x)$ and $\psi(x)$ must vanish for $x>x_0$. This, of course, does not preclude the possibility of one of these functions having already vanished at some value, say, x_1, less than x_0 (this will turn out to be the case for ψ, the proton distribution). Therefore, we proceed to seek two functions which satisfy one of the working equations for $x<x_0$, and the other equation for $x<x_1(<x_0)$ and which are taken to be identically zero for $x>x_0$ and $x>x_1$, respectively. For example, φ and ψ may satisfy (20) for $x<x_0$ and (21) for $x<x_1<x_0$ [where x_1 is determined by the solution of (21)]. In this event we would complete their definitions by taking $\varphi(x)$ and $\psi(x)$ to be identically zero for $x>x_0$ and $x>x_1$, respectively. It is seen that functions defined in this manner for all x still satisfy Eq. (20) for $x<x_0$ and Eq. (21) for $x<x_1$. But since Eq. (20) for $x>x_0$ and Eq. (21) for $x>x_1$ are not satisfied by these functions it would appear that we cannot conclude that the energy is minimized by these functions. However, as pointed out in connection with the energy variation procedure, Eqs. (20) and (21) occur multiplied by common factors, in particular $\varphi(x)$ and $\psi(x)$, respectively. Thus, one of the functions φ, ψ being zero (instead of the corresponding working equation being satisfied) is also a sufficient condition for an energy extremum.

We now have a procedure valid for all x_0 (assuming we can solve the coupled equations in the appropriate regions of x) for obtaining the desired nucleon density distribution and have the assurance that the density function, thus calculated, is physically meaningful in that it minimizes the energy of the nucleus and exhibits reasonable behavior for $x>x_0$.

Before attempting to solve the working equations for a particular value of x_0 we count the number of free input parameters in our theory. The spirit of the calculation is to treat the dimensionless parameters k, C_N, and C_C, characterizing the interaction strengths, as independent of the size of the nucleus, x_0, but permit the Lagrangian multiplier, λ (the total energy of the most energetic nucleon) to depend on x_0. The dependence of λ on x_0 (or A) implies, through Eq. (19a), that the neutron and proton Fermi levels, E_{Fn} and E_{Fp}, (or the dimensionless ϵ_{Fn} and ϵ_{Fp}) will depend on A. If we define D as the difference between the Fermi levels and make use of the difference of Eq. (19a) we see

$$D\equiv E_{Fp}-E_{Fn}=Mc^2-\beta^{-1}Mc^2$$
$$=(M_n-M_p)c^2\doteq 1.3 \text{ MeV}. \quad (22)$$

Thus, the difference between the Fermi levels is independent of A. Defining the dimensionless difference

$$\mathfrak{D}\equiv D/(p_D^2/2M),$$

we have using (19b)

$$\epsilon_{Fp}-\epsilon_{Fn}=\mathfrak{D}=\frac{1.3 \text{ MeV}}{p_D^2/2M}. \quad (23)$$

Upon examination of the working equations [(20) and (21)] there would appear to be five input parameters, k, C_N, C_C, ϵ_{Fp}, and ϵ_{Fn}. However, the method of solution employed will, for each value of x_0 selected, determine a value for ϵ_{Fn} and, hence, knowledge of the constant p_D, in (23), would give the value of ϵ_{Fp} for that x_0. Thus, specification of the four parameters k, C_N, C_C, and p_D permits solution of the working equations for the functions $\varphi(x)$ and $\psi(x)$ for arbitrary values of nuclear radius x_0.

The question then arises as to whether these four parameters [and the solutions $\varphi(x)$ and $\psi(x)$] are sufficient for determining all derived quantities such as the total energy of the nucleus, nuclear radius, etc. For example, looking at Eq. (13), we find, in addition to the above four parameters, the quantity r_D, and Eqs. (2) and (3) involve the quantity U_0. Not all these quantities are independent. In fact, of the five quantities C_N, C_C, p_D, r_D, and U_0 only three are independent as can be seen from Eqs. (10b). Thus, we have exactly *four free input parameters* in our theory: k and any three of the five quantities C_N, C_C, r_D, p_D, and U_0, with which to attempt to fit nuclear energies, neutron/proton ratios, radii, and surface thicknesses over the whole range of nuclei (excluding the lightest, which are not expected to be subject to such a purely statistical theory).

Suppose for definiteness we select the input parameter set: k, r_D, C_N, and C_C. The other quantities p_D and U_0

are then expressible, through the use of Eqs. (10b) as

$$p_D=(3\pi\hbar^3/8Me^2)(C_C/r_D^2),$$
$$U_0=(2e^2/r_D)(C_N/C_C). \tag{24}$$

We could guess values for the four input parameters, solve the working equations and compare the values of the derived quantities, e.g., total binding energy, with the experimental values for the same nucleus, then repeat the process with new guesses for the parameters. The disadvantage of this direct approach is the lack of *a priori* knowledge concerning the approximate values of the free parameters, in particular C_N, p_D, and k. An alternative is to attempt to relate some of our free parameters to more familiar quantities. The quantities employed in I, in describing infinite nuclear matter, are convenient for this purpose.

To obtain such relations, we examine our working equations [(20) and (21)] in the limit of nucleons being dynamically equivalent. That is, we retain the possibility of placing four nucleons in the same momentum state but set

$$C_C=0 \tag{25a}$$

("protons" are now chargeless), and

$$\beta=1 \tag{25b}$$

(neglect np mass difference).

From Eq. (22) we see that $\beta=1$ implies $E_{Fp}=E_{Fn}$ so we can write just ϵ_F for both ϵ_{Fn} and ϵ_{Fp}. For dynamically equivalent nucleons we expect the neutron and "proton" spatial densities to be the same, and upon examining Eqs. (20) and (21) we see that in the limit of Eq. (25) either equation is just the other equation with φ and ψ interchanged. Thus, the coupled equations do indeed permit the symmetrical solution $\psi(x)=\varphi(x)$, where φ satisfies the single equation

$$\varphi^2(x)=\frac{\dfrac{(1+k)C_N}{x}\displaystyle\int_0^{x_0}(e^{-|x-y|}-e^{-(x+y)})\varphi^3(y)[1-\tfrac{3}{5}\varphi^2(y)]ydy+\epsilon_F}{\dfrac{(1+k)C_N}{x}\displaystyle\int_0^{x_0}(e^{-|x-y|}-e^{-(x+y)})\varphi^3(y)ydy+1}. \tag{26}$$

This equation with $(1+k)C_N=C$ is the equation studied in I. There the equation was applied to infinite nuclear matter, i.e., to nuclei with arbitrarily large radii and uniform density. In this limit [φ being a constant, say, φ_∞ ($\equiv p_{F\infty}/p_D$), $\epsilon_F=\epsilon_{F\infty}$, and $x_0\to\infty$] Eq. (26) can be simplified and rearranged to give

$$\epsilon_{F\infty}=\varphi_\infty^2-2(1+k)C_N\varphi_\infty^3[1-(8/5)\varphi_\infty^2]. \tag{27}$$

Also, the ratio of the total energy to the total number of nucleons is in this same limit,

$$\bar{\epsilon}_\infty=(3/5)\varphi_\infty^2-(1+k)C_N\varphi_\infty^3[1-(6/5)\varphi_\infty^2], \tag{28}$$

where, in analogy with (19b), we have defined

$$\bar{\epsilon}_\infty\equiv\bar{E}_\infty/(p_D^2/2M), \tag{29}$$

$\bar{E}_\infty$ being the average energy per nucleon in nuclear matter. We introduce a length $r_{0\infty}$, the radius of the volume per nucleon in infinite nuclear matter. In the usual fashion

$$p_{F\infty}=\left(\frac{9\pi}{8}\right)^{1/3}\frac{\hbar}{r_{0\infty}}. \tag{30}$$

Thus far, we have introduced four new quantities, $\epsilon_{F\infty}$, $\bar{\epsilon}_\infty$, or $\bar{E}_\infty$, φ_∞, or $p_{F\infty}$, and $r_{0\infty}$; and only three new equations, (27), (28), and (30) relating them. The necessary fourth equation is provided by the Hugenholtz–Van Hove theorem,[9] which states that

$$\bar{\epsilon}_\infty/\epsilon_{F\infty}=1. \tag{31}$$

We accomplish our immediate objective in three steps: First, substituting Eqs. (27) and (28) into (31) results in the equation

$$C_N=2[5\varphi_\infty(1+k)(1-2\varphi_\infty^2)]^{-1}; \tag{32}$$

second, substituting this result back into Eq. (28) where, with the help of Eqs. (29) and (30), we find

$$\varphi_\infty^2=\frac{1-0.103796\bar{E}_\infty r_{0\infty}^2}{(18/5)-0.207592\bar{E}_\infty r_{0\infty}^2}, \tag{33}$$

(where $\bar{E}_\infty$ is in MeV); and third, using Eqs. (10) and (30),

$$C_C=\frac{3}{2}\frac{e^2}{r_D}\left(\frac{8}{9\pi}\right)^{2/3}\frac{2M}{\hbar^2}\frac{r_D^3}{r_{0\infty}\varphi_\infty}$$
$$=(0.0448394\ \mathrm{F}^{-1})r_D^2/(r_{0\infty}\varphi_\infty). \tag{34}$$

From these three equations it is easily seen that C_N is determined by k, $r_{0\infty}$, and $\bar{E}_\infty$; while C_C is determined by r_D, $r_{0\infty}$, and $\bar{E}_\infty$. Thus, we have found a new set of four parameters, namely, k, r_D, $r_{0\infty}$, and $\bar{E}_\infty$ which are equivalent to the original set, k, r_D, C_N, and C_C.

The advantage of using the new set of input parameters is made clear by the following two observations: (i) $r_{0\infty}$ is the coefficient of the "$A^{1/3}$ law" in nuclear matter and, although not precisely known, has the approximate value 1.2 ± 0.2 F, as suggested by Hofstadter's nuclear density experiments,[10] (ii) $\bar{E}_\infty$ corresponds to the coefficient of the volume term in the semiempirical mass formula and is given by Green[11]

[9] N. Hugenholtz and L. Van Hove, Physica **24**, 363 (1958).

[10] R. Hofstadter, Rev. Mod. Phys. **28**, 214 (1956).

[11] A. E. S. Green, Phys. Rev. **95**, 1001 (1954).

as -15.74 MeV. One is tempted to use this value and treat $\bar{E}_\infty$ as known, thus reducing the number of free parameters to three. However, Ayres *et al.*[12] have recently indicated that this value may be uncertain by as much as 2 MeV per nucleon. In any event Green's value provides us with an initial guess for the parameter $\bar{E}_\infty$.

We are now ready for the central problem of this work, the solving of the coupled integral equations, (20) and (21), for finite values of x_0 and $x \leq x_0$.

Employing an iteration method of solution we rewrite the working equations, (20) and (21), for a particular value of x_0, as

$$[\varphi^{(t+1)}(x)]^2=\frac{f^{(t)}(x)+kg^{(t)}(x)+\epsilon_{Fn}{}^{(t)}(x_0)}{v^{(t)}(x)+kw^{(t)}(x)+1}, \quad (35)$$

and

$$[\psi^{(t+1)}(x)]^2=\frac{kf^{(t)}(x)+g^{(t)}(x)-h^{(t)}(x)+\epsilon_{Fn}{}^{(t)}(x_0)+\mathfrak{D}}{kv^{(t)}(x)+w^{(t)}(x)+\beta}, \quad (36)$$

where

$$f^{(t)}(x)\equiv\frac{C_N}{x}\int_0^{x_0}(e^{-|x-y|}-e^{-(x+y)})[\varphi^{(t)}(y)]^3 \times\{1-\tfrac{3}{5}[\varphi^{(t)}(y)]^2\}ydy,$$

$$g^{(t)}(x)\equiv\frac{C_N}{x}\int_0^{x_0}(e^{-|x-y|}-e^{-(x+y)})[\psi^{(t)}(y)]^3 \times\{1-\tfrac{3}{5}[\psi^{(t)}(y)]^2\}ydy,$$

$$h^{(t)}(x)\equiv\frac{C_C}{2x}\int_0^{x_0}(x+y-|x-y|)[\psi^{(t)}(y)]^3ydy,$$

$$v^{(t)}(x)\equiv\frac{C_N}{x}\int_0^{x_0}(e^{-|x-y|}-e^{-(x+y)})[\varphi^{(t)}(y)]^3ydy,$$

and

$$w^{(t)}(x)\equiv\frac{C_N}{x}\int_0^{x_0}(e^{-|x-y|}-e^{-(x+y)})[\psi^{(t)}(y)]^3ydy.$$

The hope is that with increasing t (successive iterations) $\varphi^{(t)}(x)$, $\psi^{(t)}(x)$, and $\epsilon_{Fn}{}^{(t)}(x_0)$ approach definite limits, which are to be taken as the desired solutions $\varphi(x)$, $\psi(x)$, and $\epsilon_{Fn}(x_0)$, respectively.[13] The definition of the iteration procedure is completed by specifying the initial guesses, $\varphi^{(0)}(x)$ and $\psi^{(0)}(x)$ (for $x<x_0$), and by requiring the larger of $\varphi^{(1)}(x)$ and $\psi^{(1)}(x)$ to become zero at $x=x_0$, thus determining $\epsilon_{Fn}{}^{(0)}(x_0)$. The smaller of $\varphi^{(1)}(x)$ and $\psi^{(1)}(x)$ will then become zero for some value of x, say, x_1, ($\leq x_0$) and will be taken as identically zero for all x between x_1 and x_0. Having obtained $\varphi^{(1)}$ and $\psi^{(1)}$ in this manner, we repeat the procedure to find $\varphi^{(2)}(x)$, $\psi^{(2)}(x)$, and $\epsilon_{Fn}{}^{(1)}(x_0)$. This procedure is iterated until two successive iterants are within a prespecified tolerance (we used 0.02%) of each other for all $x<x_0$.

[12] R. Ayres, W. F. Hornyak, L. Chan, and H. Fann, Nucl. Phys. **29**, 212 (1962).

[13] A typical calculation requires 15 to 20 iterations.

We select the constant φ_∞ [given by Eq. (33)] as our first guess. Thus, for $x<x_0$,

$$\varphi^{(0)}(x)=\psi^{(0)}(x)=\varphi_\infty. \quad (37)$$

RESULTS AND DISCUSSION

Before reporting the numerical results[14] we submit an outline of the procedure followed for the purpose of "optimizing" the input parameters, k, r_D, $r_{0\infty}$, and $\bar{E}_\infty$. The routine employed was: (i) Choose arbitrary trial values for the input parameters (we started with $k=1$, $r_D=1.4$ F, $r_{0\infty}=1.2$ F, and $\bar{E}_\infty=-15$ MeV/nucleon). (ii) Use Eqs. (23) and (24) to calculate $\mathfrak{D}$ and Eqs. (32)–(34) to calculate C_N and C_C. (iii) Substitute k, $\mathfrak{D}$, C_N, and C_C into the iteration Eqs. (35) and (36). (iv) Select a value of x_0 (a particular nucleus) and with the aid of a digital computer solve these equations for the functions $\varphi(x)$, $\psi(x)$, and the constant $\epsilon_{Fn}(x_0)$. (v) Compute the binding energy per nucleon for the nucleus by substituting (another computer operation) the solutions $\varphi(x)$, $\psi(x)$ into Eqs. (11)–(13) and calculating the negative of the ratio of Eq. (13), E_T, to the sum of Eqs. (11) and (12) (total number of nucleons in the nucleus considered). (vi) Find the ratio of neutrons to protons by dividing Eq. (6) by Eq. (7). (vii) Repeat steps (iv)–(vi) for various values of x_0, thus obtaining theoretical curves for the variation of binding energy per nucleon and the neutron-proton ratio as a function of the nucleon number, which can be compared to available experimental curves. (viii) Repeat steps (i)–(vii) with a different choice of parameter values[15]; and continue this procedure in search of input parameter values which "best fit" the experimental data in the sense of a least-squares computation.[16]

The search produced the following best input parameter values

$$\begin{aligned} r_D&=0.56 \text{ F},\\ r_{0\infty}&=1.20 \text{ F},\\ k&=1.35,\\ \bar{E}_\infty&=-15.6 \text{ MeV}. \end{aligned} \quad (38)$$

The effective Yukawa force-range r_D is less than half (40%) of the value ($\hbar/m_\pi c$) expected on the basis of a purely single-pion exchange picture of the nucleon-nucleon force. It suggests that multiple-pion exchanges may be important, and is consistent with the fact that hyperons, which cannot interact with nucleons by single-pion exchange, nevertheless seem to be bound in hypernuclei to nearly the same extent as a nucleon would be bound. The radius of the volume per nucleon in nuclear matter, $r_{0\infty}$, is quite of the expected size. The

[14] In the following, for brevity, the predictions of the present model will be referred to as the "theoretical predictions."

[15] The method of choosing different parameter values consisted of employing a simple variation of the "grid search" technique.

[16] The sum of the squares of the differences between theoretical and experimental values divided by the number of compared values.

unlike-nucleon effective force is about $\frac{4}{3}$ as effective ($k=1.35$) as the unlike one, but we know of no rationale for a ratio near $\frac{4}{3}$.

The asymptotic energy-per-nucleon ($\bar{E}_\infty=-15.6$ MeV) is close (within 1%) to the Green[11] value, and suggests that the fears expressed[12] about this number may be somewhat alarmist. Our value of $\bar{E}_\infty$ is uncertain by about 1% because the best fit to the experimental data is not very sensitive to $\bar{E}_\infty$. The uncertainty in $\bar{E}_\infty$ causes the other parameter values also to be uncertain, as can be seen from the following list of the values of the parameters for three different good fits:

$\bar{E}_\infty$	k	r_D	$r_{0\infty}$	
−15.8	1.335	0.553	1.174	
−15.6	1.348	0.564	1.202	(39)
−15.4	1.355	0.572	1.229.	

The best fit corresponds to the middle set of values, as given before, but the fits obtained with the other two sets of values are nearly as good. That is, the mean square deviation, based on the deviations from the data (binding energy and neutron/proton ratio) computed at five or six points (spaced between A equal roughly 40 and 200), was slightly lower for the middle set of values. When only a few points of comparison are employed (as was done) to determine the mean-square deviation the resultant value will be somewhat dependent on the particular comparison points chosen. Thus, a more accurate determination of the optimum values of the parameters would necessitate the use of a larger number (≈ 20) of comparison points.[17]

Using the values of the four parameters, Eq. (38), we find

$$\begin{aligned} \varphi_\infty &= 0.6351, \\ C_N &= 1.388, \\ C_C &= 0.01866, \\ T_{F\infty} &= p_{F\infty}^2/2M = 33.33 \text{ MeV}, \\ p_D^2/2M &= 82.6 \text{ MeV}, \\ U_0 &= 379.3 \text{ MeV}. \end{aligned} \tag{40}$$

Note that the critical momentum p_D is substantially larger than the Fermi momenta involved (φ and ψ are well below unity) so that "the amount of momentum dependence needed in the interaction is not large." We are probably not in a position to distinguish, for instance, between $G(q)=1-q^2$ and $\exp(-q^2)$, which momentum dependence would not change the interaction from attraction to repulsion for any relative momentum.

As in I we can compare our results in the infinite nucleus case to the nuclear matter effective-mass approximation of Weisskopf[4] and Mittelstaedt,[7] wherein it is assumed that the energy of a nucleon with momentum p can be expressed as

$$E(p)=p^2/2M+V_0+(p/p_{F\infty})^2V_1. \tag{41}$$

Evaluating Eq. (2) in the limit of nucleons being dynamically equivalent, $\varphi(x)=\varphi_\infty$ and $x_0\to\infty$, we find

$$\begin{aligned} V_0&=-2(1+k)C_NT_{F\infty}\varphi_\infty(1-\tfrac{3}{5}\varphi_\infty^2), \\ V_1&=2(1+k)C_NT_{F\infty}\varphi_\infty^3. \end{aligned} \tag{42}$$

Introducing the effective nucleon mass, M^*, defined such that $E(p)=p^2/2M^*+V_0$, we find for the ratio of effective to free mass

$$M^*/M=(1+V_1/T_{F\infty})^{-1}=[1+2(1+k)C_N\varphi_\infty^3]^{-1}. \tag{43}$$

The values given in Eq. (40), when substituted into Eqs. (42) and (43) give

$$\begin{aligned} V_0&=-104.6 \text{ MeV}, \\ V_1&=55.7 \text{ MeV}, \\ M^*/M&=0.375. \end{aligned} \tag{44}$$

These values differ only slightly (since we found $T_{F\infty}=33.33$ compared to their input value of $T_{F\infty}=38$ MeV) from the values given by Weisskopf and Mittelstaedt for the case of vanishing rearrangement energy ($\Delta=0$) which is the same as separation energy equal to the negative of the Fermi energy ($S=-E_F$).

A comparison with the optical model is afforded by writing Eq. (41), using the values in Eq. (44) as

$$E(p)=T-104.6+55.7T/T_{F\infty}, \tag{45}$$

where T is the kinetic energy $p^2/2M$. Now consider a nucleon (neutrons and protons dynamically equivalent again) of zero total energy in nuclear matter where it sees an optical potential,[18] whose real part we call V, and has kinetic energy $T=-V$. We can calculate V by setting $E=0$ in Eq. (45), substituting $T_{F\infty}=33.33$ MeV, as given by Eq. (40), and solving for T which gives $T=39.2$ MeV and, therefore, we have[19]

$$V=-39.2 \text{ MeV},$$

which is roughly 7% below the current 42-MeV estimate based on low-energy neutron scattering.[18]

Table I shows some of the properties of the solutions $\varphi(x)$, $\psi(x)$ for various values of x_0 (all x values are measured in units of $r_D=0.564$ F).[20] Column 2 gives the

[17] Another serious limitation on the accuracy of the parameters is accuracy of the solutions φ, ψ of the working equations. To hold down the computer time needed, we settled on a one-hundred point division of the interval x_0 for purposes of numerical integration.

[18] A. E. Glassgold, *Progress in Nuclear Physics*, edited by O. R. Frisch (Pergamon Press Inc., New York, 1959), Vol. 7, Chap. 4.

[19] For comparison the first and third sets of parameter values given in Eq. (39) would yield optical potentials of 41.0 and 37.6 MeV, respectively.

[20] In I the range of investigation of x_0 was from 4.5 to 10. The parameter r_D was not determined by the work in I but was arbitrarily taken as the Compton wavelength of the π meson (=1.4 F). This assumption implied that the range of x_0 corresponded to $30<A<1100$. The smaller value of r_D determined by this work (0.564 F) forces a rescaling of the distance ($r=xr_D$) and indicates that the actual range of A studied in I was only from approximately 4 to 76. The absence of saturation for "low" A noted in I is now better understood in view of our present knowledge as to how "low" A really was.

TABLE I. Properties of the solutions $\varphi(x)$ and $\psi(x)$ for various values of χ_0 (nuclear radius). All lengths are given in units of r_D.

x_0	A	$\varphi(0)/\varphi_\infty$	$\psi(0)/\varphi_\infty$	zero diff	x_{90-10}	$x_{1/2}$	x_{0e}
16	241.43	1.029	0.884	0.96	2.72	13.75	13.80
15.5	219.87	1.030	0.893	0.93	2.75	13.29	13.31
15	199.43	1.031	0.902	0.90	2.79	12.83	12.83
14.5	180.10	1.031	0.911	0.87	2.83	12.37	12.35
14	161.88	1.032	0.920	0.70	2.87	11.91	11.86
13.5	144.77	1.032	0.928	0.675	2.92	11.45	11.39
13	128.77	1.033	0.936	0.650	2.96	10.98	10.91
12.5	113.87	1.033	0.944	0.625	3.00	10.52	10.43
12	100.03	1.033	0.952	0.48	3.04	10.05	9.95
11.5	87.26	1.033	0.959	0.46	3.09	9.57	9.48
11	75.53	1.033	0.966	0.44	3.13	9.10	9.00
10.75	70.05	1.033	0.969	0.43	3.15	8.86	8.77
10.5	64.83	1.033	0.972	0.315	3.17	8.62	8.53
10.25	59.85	1.033	0.976	0.3075	3.18	8.36	8.29
10	55.11	1.033	0.979	0.30	3.19	8.15	8.06
9.75	50.61	1.032	0.982	0.2925	3.20	7.91	7.82
9.5	46.35	1.032	0.984	0.285	3.21	7.67	7.59
9.25	42.32	1.032	0.987	0.2775	3.22	7.43	7.35
9	38.52	1.032	0.990	0.18	3.23	7.19	7.12
8.5	31.57	1.030	0.994	0.17	3.23	6.70	6.65
8	25.46	1.029	0.998	0.16	3.22	6.22	6.18
7.5	20.16	1.027	1.001	0.075	3.20	5.73	5.72
7	15.62	1.023	1.002	0.070	3.15	5.25	5.26
6.5	11.77	1.019	1.002	0.065	3.09	4.76	4.80
6	8.57	1.011	0.999	0	2.99	4.27	4.34
5.5	5.97	1.000	0.991	0	2.86	3.78	3.88

total number of nucleons [Eqs. (11) plus (12)] in the nucleus. Column 3 indicates that the neutron density [Eqs. (1a) and (10a)] near the center of the nucleus is saturated, since $\varphi(0)$ is essentially independent of the size of the nucleus, at a value slightly above the neutron density of an infinite (with no Coulomb effect and no np mass difference) nucleus. Due to the Coulomb repulsion, we would expect the addition of protons to a nucleus to cause the inner protons to spread out, lowering the density. That this is the case is shown by column 4 where it is seen that for large A the inner proton density becomes significantly less than the "proton" (=neutron) density in infinite nuclear matter. Column 5 lists the difference in extent (in units of r_D) of the neutron and proton density distributions. Since we divided the distance x_0 into 100 parts for the numerical computation, the point at which the proton density vanishes is known only to within a scale division ($0.01x_0$). Thus, the figures in column five are uncertain, in particular, each value is only known to lie between the value listed, and that value plus $0.01x_0$. The result that the neutron distribution has the greater extent was predicted by Johnson and Teller.[21]

Column 6 reports the surface thickness,[10] the distance over which the total nucleon density decreases from 90 to 10% of its central value. Our results show a surface thickness roughly independent of A, averaging to

$$\text{"90\%}-10\%\text{"}=(2.98\pm0.26)r_D=1.68\pm0.15\text{ F}. \quad (46)$$

This result is of the same order of magnitude, but somewhat lower than the lowest values for the skin thickness quoted by Preston.[22] Certainly the surface region of the nucleus is treated inadequately by the present simple model, which in effect neglects quantum-mechanical diffuseness (and can thus give a sharp edge). A tail of nucleon-distribution extending beyond our "nuclear radius" is to be expected, and it is, therefore, satisfactory that our calculated surface thickness is on the low side. It may be worth mentioning that the 90–0% surface thickness in the present model is much more nearly A-independent (than the 90–10% thickness) and averages to the lowest skin thickness (2.20 ± 0.03 F) reported by Preston.

Column 7 gives the value of x at which the total nucleon density is equal to half of its central value. This value will be referred to as the half-density radius. Column 8 gives the extent x_{0e} of the "equivalent uniform density model" (density throughout same as calculated central density and same number of nucleons).

Our results predict that the radius (as used in this paper) of the neutron distribution, x_0, exceeds the radius of the proton distribution, the difference increasing monotonically as a function of A to the value 0.54 F at $A=240$. Experimental evidence concerning the difference in the extents of the neutron and proton distributions has been presented by Elton[23] and his conclusion is that, for heavy nuclei ($A>150$), a difference between the neutron and proton half-density radii of more than 0.1 to 0.2 F is incompatible with experiment. For our solution of largest A ($=241$: $x_0=16$), we find by examining the solutions φ and ψ that the neutron density drops to half its central value at $x=13.85$, while the proton density becomes half its central value when $x=13.61$. Thus, the difference in the

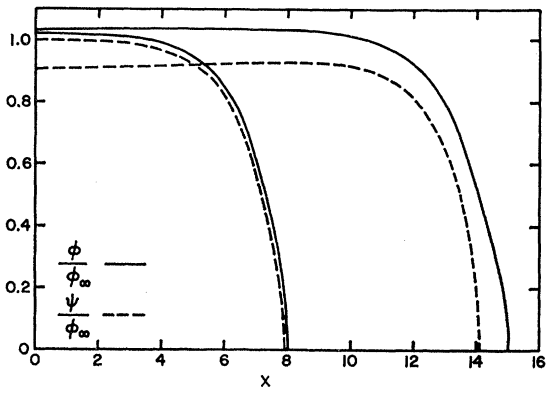

FIG. 1. The variation of φ and ψ (the Fermi neutron and proton momenta in units of p_D) as a function of x (the radial distance in units of r_D) for $x\leq x_0$. Curves are given for x_0 (the nuclear radius in units of r_D) equal to 8 and 15, corresponding to $A=25$ and 200. φ_∞ is the Fermi momentum (in units of p_D) of a nucleon in infinite nuclear matter.

[21] M. H. Johnson and E. Teller, Phys. Rev. **93**, 357 (1954).

[22] M. A. Preston, *Physics of the Nucleus* (Addison-Wesley Publishing Company, Inc., Reading, Massachusetts, 1962), p. 46.

[23] L. R. B. Elton, Nucl. Phys. **23**, 681 (1961).

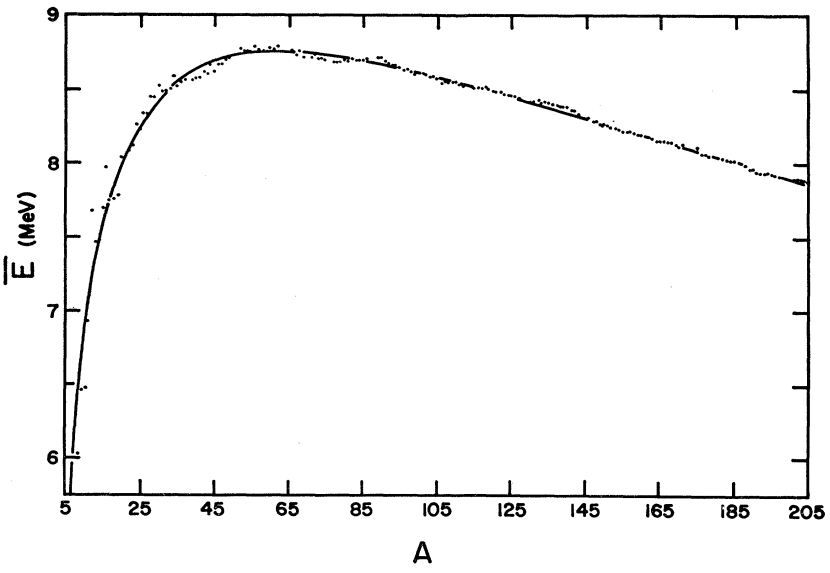

FIG. 2. The variation of $\bar{E}$, the binding energy per nucleon, as a function of A. The solid curve represents the theoretical values, the isolated points the experimental values.

np half-density radii is $0.24r_D$ or 0.135 F, which is well within Elton's requirement.

Figure 1 displays the solutions $\varphi(x)$ (solid curve) and $\psi(x)$ (dashed curve) as functions of x for two values of x_0, 8.0 and 15.0, corresponding to $A=25$ and 200 [we have normalized the solutions to the infinite nucleus value by multiplying by φ_∞^{-1} $(=1.573)$]. For small A the solutions φ and ψ are nearly equal, but as A increases the Coulomb energy rises rapidly ($\propto Z^2$) and, thus, the proton density distribution ($\propto\psi^3$) looks considerably different (lower in central density and lesser in spatial extent) from the neutron distribution ($\propto\varphi^3$). It is to be remembered that although, as in Fig. 1, as $x\rightarrow x_0$, $\varphi\rightarrow 0$ with infinite slope, the density $\rightarrow 0$ with zero slope (cf. Fig. 2 in I). Some conclusions that follow from Fig. 1 (inner neutron density being saturated, etc.) have already been drawn from Table I. There is, however, one more result to be emphasized. Although the neutron density distribution decreases monotonically as a function of x for all A, the proton distribution does not. In particular, for $A>55$ the proton density dips slightly in the center; that is, its maximum is displaced from the center of the nucleus (compare the two dashed curves in Fig. 1). Quantitatively, for $A=55$ $(x_0=10)$, the point of maximum proton Fermi momentum (and, therefore, proton density) is displaced from the center of the nucleus by $0.10x_0$ $(=0.56$ F) and has a value 0.0001% greater than the central Fermi proton momentum. For $x_0=15$ $(A=200)$ the maximum of the proton Fermi momentum occurs at $x=0.55x_0$ and is noticeably (2.3%) greater than the proton Fermi momentum at the center of the nucleus. A dip of 2.3% in proton Fermi momentum corresponds to a dip of almost 7% in proton density. As A increases both the amount of dip and the amount of departure of the proton density maximum from the center of the nucleus increase as is to be expected since both effects are directly attributable to the increase in Coulomb repulsion energy.

In Fig. 2 is exhibited the variation of the binding energy per nucleon, $\bar{E}$, as a function of the number of nucleons, A. The smooth curve gives the theoretical values of $\bar{E}$. The isolated points indicate the experimental values of $\bar{E}$ for all known stable nuclei having A between 5 and 205 (when more than one experimental value of $\bar{E}$ is available for a particular value of A only the average value is shown in Fig. 2). It is seen that the theoretical curve accurately represents the over-all "smoothed-out" behavior of the experimental data reproducing the average of the experimental values to well within 1% for nearly all A in the range 5 to 205. The success of our theory in not only satisfying the general requirement of exhibiting saturation, but in reproducing to high accuracy the observed binding energies for all A is, indeed, gratifying. In fact, it probably should be admitted that this fit seems suspiciously good, in view of the fact that we have made no effort to exclude aspherical nuclei from those to which the fit is made.

Figure 3 presents the neutron-proton ratio, N/Z, as a function of A. The theoretical values are represented by the smooth curve. The N/Z values of the experimentally known stable nuclei are plotted as isolated points. Except at very low A, the theoretical curve can be accurately represented by the Weizsäcker expression[11]

$$N/Z=1+0.015A^{2/3}, \tag{47}$$

since for $A>35$ these two curves differ by less than 0.14%. At lower A, for example, at $A=12$, the theoretical curve is about 1% below the value given by Eq. (47), and for $A<12$ the difference is greater than

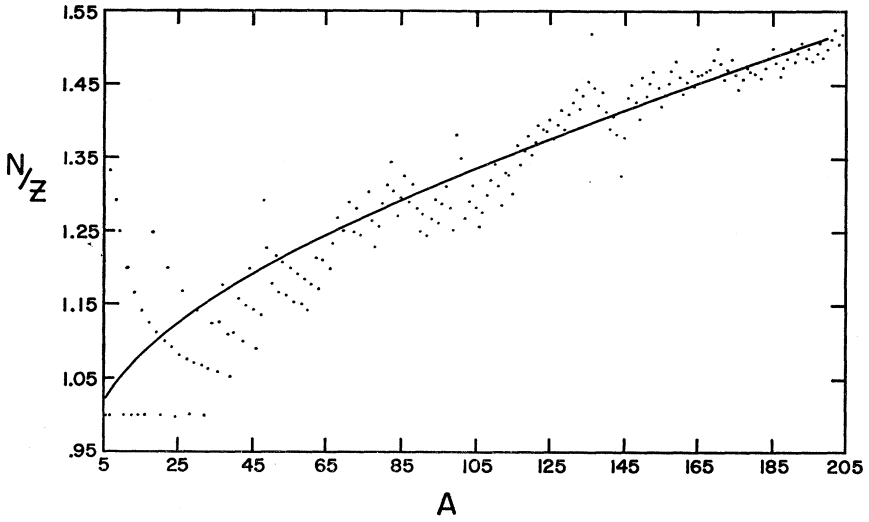

FIG. 3. The variation of the neutron-proton ratio, N/Z, as a function of A. The solid curve gives the theoretical values, the isolated points the experimental values (averaged for each A).

1%. The same information is presented in slightly different form in Fig. 4, where N is plotted as a function of Z. The smooth curve gives the theoretical values and the isolated points the experimental values (Fig. 4 contains information in the A range 205 to 240 not exhibited in Fig. 3). The fit is seen to be very satisfactory over the whole range of A.

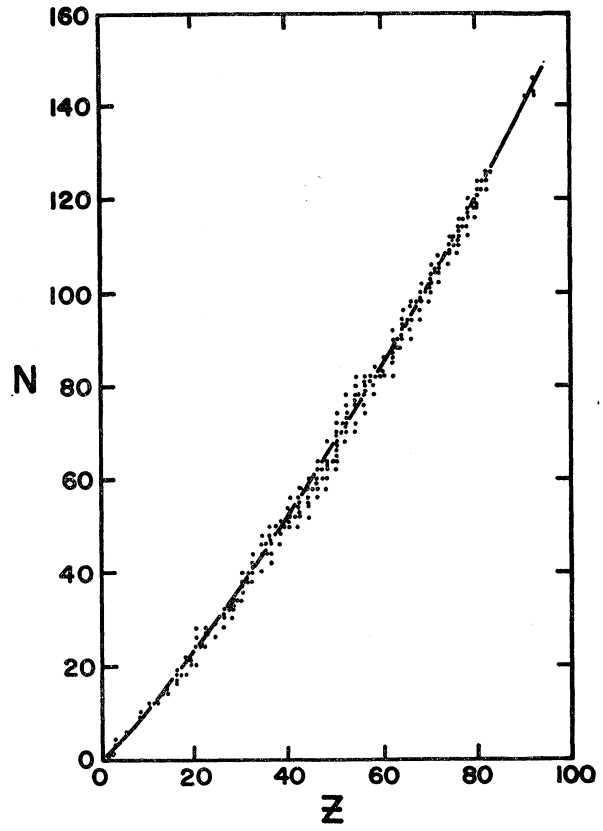

FIG. 4. Theoretical (solid curve) and experimental (isolated points) values of N as a function of Z.

The upper set of data in Fig. 5 shows x_0 plotted as a function of $A^{1/3}$. We have indicated on the figure an attempt to fit the data with a (not necessarily the best) straight line, whose equation is $x_0=2.48A^{1/3}+1.00$, or multiplied by r_D, $R=1.40A^{1/3}+0.56$ F. The departures from the given line indicate that to fit the points at very high A a line having greater slope (the slope in the $A^{1/3}$ "law" is usually designated by the symbol r_0) is needed (e.g., at $A=240$, $r_0\doteq 1.48$ F), whereas to fit the low A portion a much lower value of r_0 is needed (e.g., at $A=5$, r_0 would need to be $\doteq 1.16$ F). Thus, we see that a unique value of r_0 does not exist. The variation of slope (r_0), over the range of A considered, can be summarized by the statement $r_0=1.32$ F$\pm 12\%$.

The lower set of data in Fig. 5 presents x_{0e} (the extent of the equivalent uniform density model) as a function of $A^{1/3}$. As before, to illustrate the departure of the data from a straight-line fit we have included the line $x_{0e}=2.15A^{1/3}$ or $R_e=1.21A^{1/3}$ F. If we require the line to pass through the origin (as one would expect for a uniform density model) we see that for medium A a lower slope is needed (e.g., $A=22$ slope $\doteq 1.185$ F), while for very large A a larger value of slope is required (e.g., $A=240$, slope $\doteq 1.25$ F).

We conclude that both sets of data in Fig. 5 show about the same departure from straight-line fits and that the slope (r_0) of a straight-line fit to the upper (x_0) data may exceed, by as much as 15%, the slope of a similar fit to the x_{0e} data. These facts indicate the necessity for caution when attempting to compare directly r_0 values based on different models.

The deviation from the $A^{1/3}$ law, observed in Fig. 5, can be explained by plotting x_0 as a function of $N^{1/3}$, as is done in Fig. 6. It is seen that in this case the data can be well represented by a straight-line fit. The equation of the line drawn in Fig. 6 is $x_0=2.74N^{1/3}+1.47$ which when multiplied by r_D ($=0.564$ F) becomes

$$R=1.54N^{1/3}+0.83 \text{ F}. \tag{48}$$

Now if N can be expressed as A multiplied by a constant (for nuclear matter $N=A/2$) we arrive at a linear $A^{1/3}$ dependence. However, because of the Coulomb energy, the ratio N/A is itself a function of A and, therefore, r_0 will be A-dependent. We are in a position to predict this A dependence since we have in Eq. (47) an analytic expression which accurately (except for very low A) approximates N/Z as a function

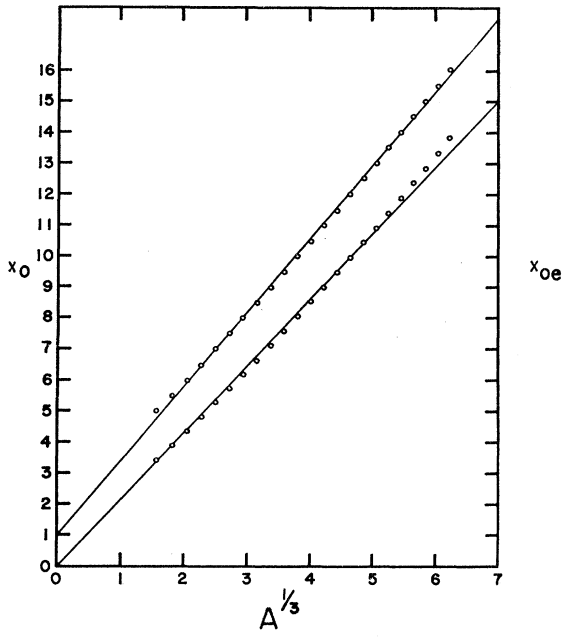

FIG. 5. The points present χ_0 (nuclear radius) and the lower points, χ_{0e} (radius of equivalent uniform density model), as a function of $A^{1/3}$. Equations of the "fit" lines are given in text.

of A. We find[24] (in F)

$$R=1.22\left(\frac{1+0.015A^{2/3}}{1+0.0075A^{2/3}}\right)^{1/3}A^{1/3}+0.83.$$

[24] Equation (32) of I reads $R=1.00r_{0\infty}A^{1/3}+1.67r_D$ which when evaluated using present values of $r_{0\infty}$ and r_D becomes $R=1.20A^{1/3}+0.94$ F.

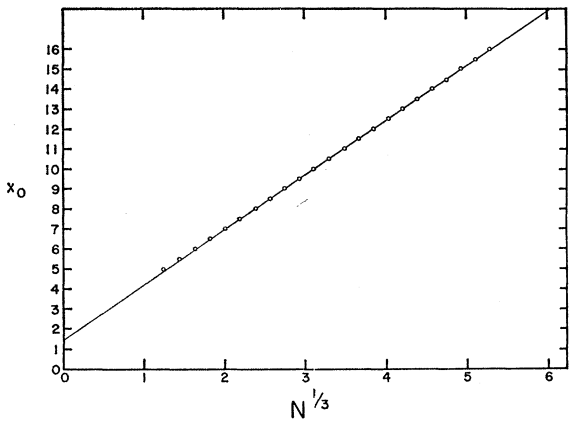

FIG. 6. The variation of x_0 as a function of $N^{1/3}$, N being the neutron number.

CONCLUSION

A credible zero-order nuclear model is given by treating attractive but velocity-dependent two-body interactions in Thomas-Fermi approximation. Such a model reproduces the gross energetics and sizes given by experiment for reasonable values of a small number of input parameters. The model predicts a small but definite Johnson-Teller effect: The neutron distribution extends out beyond the proton distribution. It also predicts a definite depression of the central proton density for medium and heavy nuclei. The treatment of the extremities of the neutron and proton distributions in this model is certainly not accurate. There is no way that this model can deal directly with a possible clustering effect far out in the nuclear surface. The sharp edge of the nucleus predicted by a Thomas-Fermi model with finite-range forces is certainly unrealistic, but we see no evidence that it is fatal to the model or responsible for the prediction of a spurious Johnson-Teller effect.

ACKNOWLEDGMENTS

The AEC computing facility at New York University made many hours of IBM 704 computing time available to us. The Research Committee of the University of Wisconsin supplied WARF funds for some direct support and for CDC 1604 computer time.